Spatiotemporal instability in a diffusively relaxed dynamics

Syed Shahed Riaz[*]

Department of Chemistry, Rama Krishna Mission Vidyamandira, Belur Math, Howrah 711202, India

The diffusion equation fails to offer a satisfactory description of dynamics when the correlation between successive motions of dispersive particle is large. Further, the equation is associated with the pitfall of predicting the infinite propagation speed of the diffusive particles. Both limitations arise as the Brownian picture (on which the equation is based on) does not take into account the inertia of the diffusive particles. This could be overcome by introducing a delay in the diffusive flux. The resultant delay-diffusion equation may be converted to an ordinary differential equation by linearizing the flux with respect to the delay, a technique valid in general for small delays. In this article I show that the condition for a spatial bifurcation induced by diffusive delay in the delay differential model is significantly different from the condition derived in an earlier work modifying the reaction-telegraphic equation based on a microscopic approach. The latter necessitates criteria not realizable in common reaction-diffusion models and therefore effectively rules out such kinds of instability in these models. I show here that the instability condition derived with the original nontruncated version of the delayed reaction-diffusion equation does not impose any constraint on the model kinetics, but only requires the diffusive memory to be large enough. Numerical simulation with three well-known reaction-diffusion models corroborates with the predictions of the linear analysis and ensures the that spatiotemporal structure generated is stable in the long term.

I. INTRODUCTION

The diffusion equation is universally employed to describe the dynamics of particles moving under Brownian motion and is associated with the pitfall of predicting a zero relaxation time for the flux and, consequently, infinite propagation speed of the diffusing particles. This is evident from the Gaussian solution of the said equation given as

$$F(r,t) = \frac{1}{(4\pi Dt)^{\frac{1}{2}}} \exp\left(-\frac{r^2}{4Dt}\right),$$

which ensures nonzero value of particle density $F(x,t)$ at any distance from the origin, at any arbitrary time instant, however small, even if all the particles were initially localized at the origin. Such discrepancy originates for not taking into account the inertia of the Brownian particles and therefore can be eliminated through invoking a nonzero relaxation time of the flux in the original Fick's law of diffusion (the Cattaneo modification [1]),

$$J(r, t+\tau) = -D \frac{\partial u(r,t)}{\partial r}. \tag{1}$$

The resultant delay differential equation can then be reduced to ordinary differential equations expanding the flux in Taylor series truncating at the linear term,

$$J(r,t) + \tau \frac{\partial J(r,t)}{\partial t} = -D \frac{\partial u(r,t)}{\partial r}. \tag{2}$$

Originally proposed to eliminate the paradox of instantaneous propagation of energy in the case heat of transport,

the Cattaneo modification of Fick's law has already been extensively applied to a wide range of processes involving both mass and energy transports. Instances include propagation of shock waves in rigid heat conductor [2], oscillatory Rayleigh-Benard convection [3], and evolution of viscous cosmological models [4–6]. In general, the diffusion equation, which is based on a Brownian picture of motion, fails to offer an accurate description of the dynamics when the dispersion of particles are not mutually independent and the individuals have well-defined velocities. The delay in the flux equation may be viewed as a measure of the correlation between successive movement of the diffusing particles. The correlation depends on the mean free path of collision; the larger the mean free path, the stronger the correlation (for a detailed discussion see Ref. [7]). In liquids, where the mean free path is small, only a fraction of the molecular diameter, the inertia, or the temporal correlation of the instantaneous velocities are negligible even on mesoscopic scales, and the velocities are not accurately defined in the molecular scales. Dispersal dynamics is then governed by random motions of the particles and the reaction-diffusion equation offers a fairly satisfactory picture of chemical reactions in aqueous solutions. However, for particles dispersing in dilute gases, the mean free path could be several orders of magnitude larger than the molecular diameter, so the inclusion of finite memory seems to be necessary. Also since micro-organisms and animals have the tendency to continue moving in the same direction in successive time intervals, models including nonzero relaxation gives a better description for spatial spread of population than the often-used diffusion equation. Furth [8] applied his theory of delayed diffusive flux to experiments on the motion of bacteria.

―――――――
[*]shahedrz@gmail.com

Combining Eq. (2) with reaction kinetics, we obtain the reaction-telegraphic or the reaction-Cattaneo equations,

$$\tau \frac{\partial^2 u(r,t)}{\partial t^2} + [1 - \tau f'] \frac{\partial u}{\partial t} = D \frac{\partial^2 u(r,t)}{\partial r^2} + f(u). \quad (3)$$

The parameter τ, for the case of thermal conduction, characterizes thermal inductance, interpreted as the time needed for the thermal energy to accumulate before it propagates. In the context of propagation of matter it can be understood as the time required for the concentration gradient to induce the diffusive flux. The range of τ widely varies; from as low a value of 10^{-10} to as high as 20 or 30 s has been observed experimentally (a discussion on the magnitude of τ and its physical significance may be found in Ref. [9]). The reaction-Cattaneo equation was derived without the aid of assuming smallness of τ, under special circumstances [10], but generally follows from the linearization of flux in Eq. (1) and therefore is untenable if inertia is large. In that case, we need to work with the original delayed equation. At the microscopic level, the Cattaneo modification amounts to replacing the Brownian picture of motion with a persistent random walk. Additionally it requires the reaction at any instant to be independent of the direction of its motion of the molecules (isotopic random walk). This, however, leads to a situation which does not ensure the rate of removal or where the death of particles of a given type goes to zero as the density of these particles vanishes. This was later modified [11] by assuming the birth and death processes of molecules to be independent of the direction of motion and that the daughter particle chooses both directions with equal probabilities. Instead of kinetics terms identical to both left- and right-going particles, now we have for the two types of particles

$$f^+(u^+, u^-) = \tfrac{1}{2} b(u) - d(u) u^+, \quad (4)$$

$$f^-(u^+, u^-) = \tfrac{1}{2} b(u) - d(u) u^-, \quad (5)$$

with $b(u) \geqslant 0$ and $d(u) \geqslant 0$. With such a form of the kinetics, ultimately evolution equations (but not the usual form of the reaction-telegraphic equation, as that would additionally require the death rates to be constant) can be derived for the total density and the flow term of each species ($i = 1, 2$):

$$\frac{\partial U_i}{\partial t} + \gamma_{x_i} \frac{\partial V_i}{\partial r} = b(U_i, U_{i+1}) - d(U_i, U_{i+1}) U_i, \quad (6)$$

$$\frac{\partial V_i}{\partial t} + \gamma_{x_i} \frac{\partial U_i}{\partial r} = 2\mu_x V_i - d(U_i, U_{i+1}) V_i. \quad (7)$$

Through a linear stability analysis on (6) and (7), Horsthemke demonstrated that all the wave numbers above a given threshold become unstable if the following condition is satisfied:

$$A_{11} - d\left(U_i^0, U_{i+1}^0\right) > 2\mu_{U_1} > 0, \quad (8)$$

where A_{11} represents the first element of the stability matrix and $d(U_i^0, U_{i+1}^0)$ the decay term in the kinetic term of the activator calculated at the steady state (U_i^0, U_{i+1}^0); μ is the probability that the direction of motion of the corresponding species will be reversed per unit time. The macroscopic analog of μ is the inverse of τ that appears in the reaction-telegraphic equation. Most of the reaction-diffusion models generally studied for pattern formation (like the Lengyel-Epstein model

which is being also employed here) has the $A_{11} - d(x, y)$ term as less than zero and hence precludes any such instability. In this article we show that no such criteria on kinetic parameters limit the applicability of the analysis here when we work with the original delayed-differential model (thus adopting a purely macroscopic approach), and therefore the kind of instability proposed in this article is expected to manifest in many of the available reaction-diffusion models in wider ranges of parameter space, provided the diffusive delay is large enough. However, while for the reaction-diffusion models that represent ecological or epidemiological models or phenomena in the cosmic world the diffusive delay is often fairly large, it may not be so in the case of chemical reaction-diffusion models. So under normal circumstances it is unlikely that diffusive delay would be large enough to induce instability in the ordinary chemical reaction-diffusion models in aqueous solutions. But on macroscopic scales such as for reaction-diffusion models that involve turbulent diffusion, the application of the diffusion equation does not yield satisfactory results and one needs to consider the effect of nonzero relaxation. Hence to test the hypothesis that a memory in the diffusive flux if large enough could interfere with the stability condition of the dynamics of a real chemical reaction-diffusion model (like CDIMA, the chlorine-dioxide-iodide-malonic acid model, the one discussed here) we may require to implement a condition of turbulent diffusion. To the best of my knowledge, the effect of turbulent diffusion on a chemical reaction-diffusion system has not yet been studied experimentally in the context of spatiotemporal instability, presumably due to the difficulty of setting up and maintaining a condition for turbulent diffusion in an experimental arrangement. However, the present study indicates that this could be an area worth exploring in the context of CDIMA or any other appropriate chemical reaction-diffusion model. Another model that we employ in the study (the pigmentation model) is not phenomenological in nature but derived by expanding the reaction terms $f(u, v)$ and $g(u, v)$ around the steady state (u_0, v_0) and then retaining specific terms motivated by the requirement of conservation of certain species. The generalized structure of the model allows the inferences derived with this model to apply over a wide range of phenomena. For example, with this model, by just adjusting a couple of parameter values one may generate a structure that bears a striking resemblance to almost every skin pattern observable in fish (hence we call it the "pigmentation of fish" model). Finally, I briefly mention the results of numerical analysis with the well-known Fisher equation. The generation of instability in this model over a critical value of diffusive memory demonstrates further that the scope of the instability could be quite broad. The point to note here is that the Fisher equation, originally proposed to explain the spread of an advantageous allele in a gene population, is one of the very basic models of ecology and this, along with many of its variants, is routinely employed to study the spatiotemporal distribution of species in ecological as well as epidemiological models. The nonzero diffusive memory in such as system implies that the species takes finite time before responding to a population gradient (according to the microscopic picture, it amounts to assuming that the species always continues in a given direction by a constant distance before being ready for the next jump). This is fairly common among living species and originally Furth [8] put forward his theory of delayed diffusive flux to

experiments on the motion of bacteria. Recently Alharbi *et al.* [12] has investigated the critical domain problem of population dynamics for a logistic growth model using a reaction-telegraphic equation. Among these cases where the memory is appreciably large I hope the method described here will be more useful than the reaction-telegraphic equation for reasons elaborated above. Last, it should be mentioned here that the analysis presented in this article could point out the existence of spatial Hopf bifurcation in a system but could not distinguish between supercritical or subcritical. Numerically, we could see that the instability in the CDIMA and the pigmentation models is associated with the concentration variables oscillating in small, finite amplitudes, indicating the Hopf bifurcation to be supercritical in nature. With the Fisher model, however, the oscillations once initiated keep growing indefinitely and eventually diverge in the long run, suggesting that the nature of the bifurcation is subcritical. Finally, it should be clarified at this point that the choice of the models was not motivated by any experimental consideration but to ensure that appropriately varying parameter space, we may choose to start with any of a wide range of initial states [unstable Hopf (with CDIMA model), stable homogeneous (with the pigmentation fish model), or unstable Turing (with both)] and investigate the effect of diffusive memory on the dynamics in all these cases. The reference to the numerical results of the Fisher equation is for the purpose of presenting a model which, being representative of ecological dynamics, offers a wider range of applicability and also to discuss a case where the bifurcation is subcritical. The delay-differential model analyzed here offers a generalization to the dispersal dynamics; it reduces to the reaction-telegraphic model at small τ and Brownian motion as τ goes to zero. Thus the noninstantaneous diffusion model provides a unified treatment which covers the whole range of transport, from the diffusive limit to the ballistic limit.

Delay-differential equations have been applied to a wide range of dynamical systems encompassing physical, chemical, or biological domains over decades. Delayed feedback loops in gene regulatory networks in many cases induce Hopf bifurcation, leading to oscillations in various components responsible for a wide range of processes which includes phenomena that are both crucial to the existence of species, like developmental patterns [13], or ones detrimental to it, as in dynamical blood diseases [14]. Delay plays a pivotal role in the dynamics of other kinds of networks as well, electrical or Internet [15–17]. In the spatial domain, a delay-induced Turing bifurcation leading to stationary patterns in reaction-diffusion system has also been reported [18]. In all these cases the delay appears in the source terms, generally to account for the time taken by some steps (often unknown) not considered in the kinetic model. Theoretical and experimental studies have already demonstrated that introduction of a time delay between a trigger event and the resulting pulse may result in counterintuitive behavior in the case of a pair of diffusively coupled chemical oscillators, like in-phase synchronization in inhibitory pulse-coupled systems or out-of-phase oscillations with excitatory coupling [19]. In contrast to these works, here we consider a single chemical reaction-diffusion model with a memory in the diffusion part of the dynamics: a diffusive memory, which arises due to the inherent inertia of the diffusive particles.

Spatiotemporal structures are ubiquitous in the chemical, physical, and biological worlds, with hydrodynamics, chemical reaction-diffusion systems [20–22], epidemiology, ecology [23], and developmental biology [13,24] offering some of the best examples. While a number of mechanisms have been put forward to account for the generation of these patterns, in many cases stringent instability criteria on the kinetic parameters limits their applicability. The stability criteria for the mechanism proposed here do not include any such restraint on the kinetic parameters, only requiring diffusive memory to be appreciable. A delayed response of the diffusive flux to the concentration gradient, which would generate the diffusive memory, is fairly common in practical systems, and the current mechanism has the potential to bring a wider range of pattern-forming phenomena into mathematical modeling.

This paper is organized in two parts; in Sec. II, I derive the condition for spatial Hopf bifurcation on a generalized reaction-diffusion model that includes diffusive memory in one of the variables, without making any assumption regarding the magnitude of the memory. Subsequently, in Sec. III, the two reaction-diffusion models are simulated both in the absence and in presence of memory; the results vindicate the predictions of the analysis.

II. REACTION-DIFFUSION EQUATION WITH DIFFUSIVE MEMORY

We consider the concentration of a reacting species or field variable $u(x, t)$, a function of space x and time t in terms of a reaction-diffusion system. The reaction-diffusion equation can be constructed phenomenologically from the continuity equation with a source term $f(u)$,

$$u_t(x, t) = -J_x(x, t) + f(u), \qquad (9)$$

where $J(x, t)$ is the flux of $u(x, t)$.

As explained earlier, a generalization of the reaction-diffusion equation that includes the effect of finite memory transport is given by Cattaneo's modification of Fick's law,

$$J(x, t) = -Du_x(x, t - \tau). \qquad (10)$$

Equation (10) implies that a concentration gradient at a time (t-τ) causes a flux at a later time t, so τ is the average time for a particle to adjust its motion in a particular direction in response to the concentration gradient. In the case of any dynamics that involve memory it is always necessary to choose between a discrete delay and a distributed delay kernel. In the former case the dynamics at a given point depends on the value of the concentration variables at a fixed time in the past, while in the latter case it would depend on the entire past history. The $u(x, t - \tau)$ in (10) for a distributed delay has to be replaced by the integral $\int_{-\infty}^{t} u_x(\tau)G(t - \tau)d\tau$, where $G(t - \tau)$ is the distribution kernel for the delay. The integral reduces to a discrete value $u(x, t - \tau)$ when the distribution kernel is a δ function. In this article we consider the case of the delay to be discrete. Further, we assume it to have a fixed value throughout the dynamics in the entire space, neglecting all possible fluctuations in space or time. Using Equation (10) as a modification of Fick's law and the continuity Equation (9) we arrive at the diffusively relaxed reaction-diffusion equation

$$u_t(x, t) = D\nabla^2 u(x, t - \tau) + f(u). \qquad (11)$$

We now consider a two-variable reaction-diffusion equation which describes the dynamics of two field variables $u(x,t)$ and $v(x,t)$. The time delay τ is incorporated in the diffusion part of one of the variables, here in u,

$$u_t(x,t) = f(u,v) + \nabla^2 u(x,t-\tau),$$
$$v_t(x,t) = g(u,v) + d\nabla^2 v(x,t), \qquad (12)$$

with $f(u,v)$, $g(u,v)$ denoting the respective reaction terms and where d denotes the ratio of the two diffusion coefficients. We now consider small spatiotemporal perturbations $\delta u(x,t)$ and $\delta v(x,t)$ on a homogeneous steady state (u_0, v_0). Subsequently expanding the reaction terms around this steady state in a Taylor series up to first order, we obtain

$$\delta u_t(x,t) = f_u \delta u + f_v \delta v + \nabla^2 \delta u(x,t-\tau),$$
$$\delta v_t(x,t) = g_u \delta u + g_v \delta v + d\nabla^2 \delta v_{xx}(x,t).$$

Expressing spatiotemporal perturbation $\delta u(x,t)$ and $\delta v(x,t)$ in (13) by the usual forms

$$\delta u = \delta u_0 e^{\lambda t + ikx},$$
$$\delta v = \delta v_0 e^{\lambda t + ikx},$$

we obtain the dispersion relation:

$$\lambda^2 + b_1 \lambda + b_2 + (b_3 \lambda + b_4)e^{-\lambda\tau} = 0 \qquad (13)$$

with

$$b_1 = -(g_v + f_u) + dk^2$$
$$b_2 = f_u g_v - f_v g_u - f_u dk^2$$
$$b_3 = k^2$$
$$b_4 = -g_v k^2 + dk^4.$$

The system loses its stability to a spatial Hopf bifurcation only when a purely imaginary solution appears at a finite value of the wave number k. In that pursuit we insert $\lambda = i\omega$ into Eq. (13). Further, applying de Moivre's theorem and then separating the real and imaginary parts we finally obtain

$$\cos(\omega\tau) = \frac{(b_4 - b_1 b_2)\omega^2 - b_2 b_4}{b_3^2 \omega^2 + b_4^2},$$
$$\sin(\omega\tau) = \frac{b_3 \omega^3 + (b_1 b_4 - b_2 b_3)\omega}{b_3^2 \omega^2 + b_4^2}. \qquad (14)$$

Equation (15) implies that ω must satisfy the following equation:

$$\omega^4 + \left(b_1^2 - 2b_2 - b_3^2\right)\omega^2 + b_2^2 - b_4^2 = 0, \qquad (15)$$

where ω is real only if either of the following conditions are met:

$$\left(b_1^2 - 2b_2 - b_3^2\right) < 0, \qquad (16)$$

$$\left(b_2^2 - b_4^2\right) < 0. \qquad (17)$$

The unique solution $(\omega\tau)$ of (15) could be written as

$$\omega\tau = \arccos\left[\frac{(b_4 - b_1 b_3)\omega_l^2 - b_2 b_4}{b_3^2 \omega_l^2 + b_4^2}\right] \qquad (18)$$

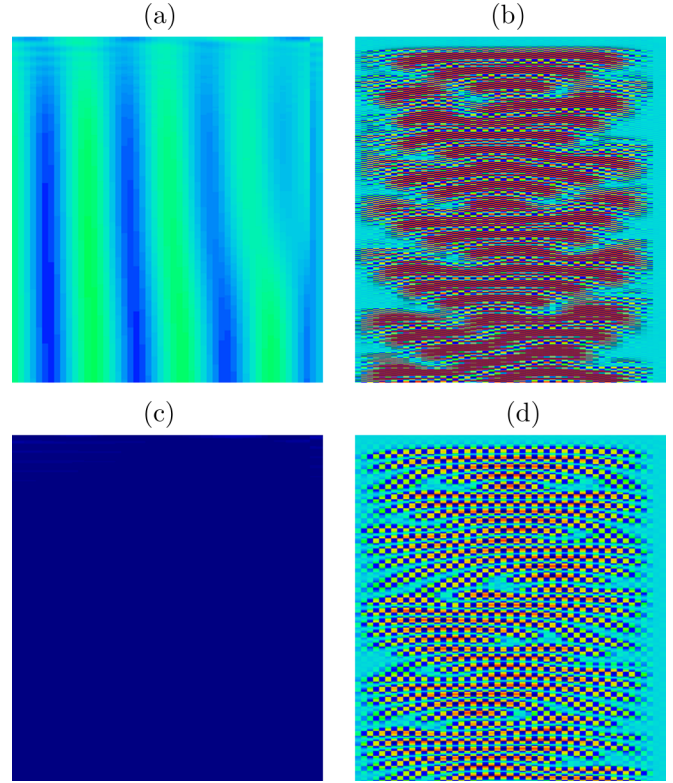FIG. 1. Figure demonstrates the space-time contour of the the variable $u(x,t)$ simulated numerically using Eqs. (22) for the parameter space: $\alpha = 0.899$, $\beta = -0.91$, $\gamma = -0.899$, $\delta = 2.0$ and (a) $d = 0.516$, $\tau = 0.0$; (b) $d = 0.516$, $\tau = 0.17$; (c) $d = 1.0$, $\tau = 0.0$; and (d) $d = 1.0$, $\tau = 0.34$. Panels (a) and (c) give the concentration distribution when the diffusive memory is not considered. Panel (a) corresponds to a Turing region, and the time is plotted along the y axis so the perpendicular stripes represent a stationary Turing structure. Panel (c) corresponds to a parameter space beyond the Turing zone, marked by a uniform distribution of species in space and time. Panels (b) and (d) are the results of simulation when diffusive memory is considered and has a value higher than the threshold inside the Turing region and beyond it, respectively. In both cases the inclusion of diffusive memory induces a spatiotemporal structure, suggesting the simultaneous occurrence of spatial inhomogeneity and temporal nonstationarity. The nature of the temporal and spatial structure are separately demonstrated in Figs. 2 and 3, respectively.

if $\sin(\omega\tau) > 0$ and

$$\omega\tau = 2\pi - \arccos\left[\frac{(b_4 - b_1 b_3)\omega_l^2 - b_2 b_4}{b_3^2 \omega_l^2 + b_4^2}\right] \qquad (19)$$

if $\sin(\omega\tau) < 0$.

Now the sequences are defined: $\tau_{2,l}^{1,j}$ and $\tau_{2,l}^{2,j}$, for $l = 1,2$,

$$\tau_{2,l}^{1,j} = \frac{1}{\omega_l}\left\{\arccos\left[\frac{(b_4 - b_1 b_3)\omega_l^2 - b_2 b_4}{b_3^2 \omega_l^2 + b_4^2} + 2j\pi\right]\right\} \qquad (20)$$

and

$$\tau_{2,l}^{2,j} = \frac{1}{\omega_l}\left\{2\pi - \arccos\left[\frac{(b_4 - b_1 b_3)\omega_l^2 - b_2 b_4}{b_3^2 \omega_l^2 + b_4^2} + 2j\pi\right]\right\}. \qquad (21)$$
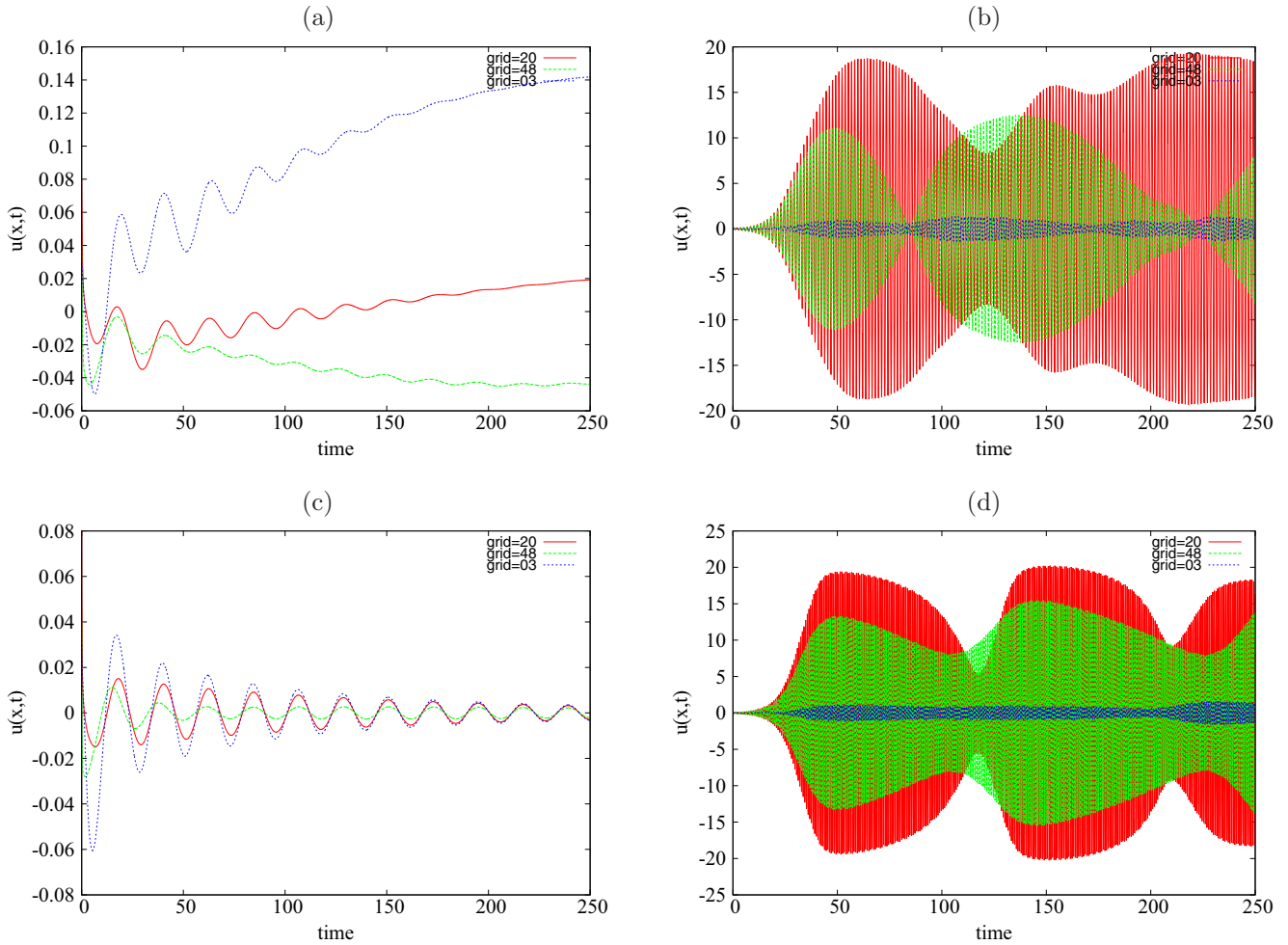
FIG. 2. Figure demonstrates the temporal evolution of the variable $u(x, t)$ simulated numerically using Eqs. (22) for the parameter space: $\alpha = 0.899$, $\beta = -0.91$, $\gamma = -0.899$, $\delta = 2.0$ and (a) $d = 1.0$, $\tau = 0.0$; (b) $d = 1.0$, $\tau = 0.17$; (c) $d = 0.516$, $\tau = 0.0$; and (d) $d = 0.516$, $\tau = 0.34$, at three arbitrarily chosen grid points. Panels (a) and (c) give the concentration distribution when the diffusive memory is not considered. Panel (a) corresponds to a Turing region, and the concentration at the three space points eventually reaches stationarity but each at a different value, as required for a stationary Turing structure. Panel (c), on the other hand, corresponds to parameter space beyond the Turing zone, and the concentration reaches the same stationary value everywhere. Panels (b) and (d) are the results of simulation when diffusive memory is considered and has a value over the threshold inside Turing region and beyond it, respectively. Evidently diffusive memory induces a complex temporal oscillation in the concentration variables in all three cases. This suggests the diffusive memory induces a supercritical Hopf bifurcation. The phase or the amplitudes of oscillation are not synchronized for the three space points, and therefore we get a spatial structure that keep changing in time, such as a complicated spatiotemporal structure as demonstrated in Fig. 1.

It follows from here (a detailed analysis may be found in Ref. [25]) for τ above a value given by any one of the above sequences (20) and (21), and Eq. (15) admits positive ω^2, provided that either of the conditions given by Eqs. (16) or (17) is satisfied. Evidently the "k^4" term in b_4 makes $b_2^2 - b_4^2$ negative for large values of k which implies that condition (17) is satisfied for any k above a minimum. The instability does not require any additional constraint on the kinetic parameters. Positivity of ω^2 for all k values above a threshold ensures there exist a pair of imaginary eigen value (λ) of opposite sign for every wave number k in this range; the condition for spatial Hopf bifurcation. Thus the diffusive memory at a value given by any of the sequences (20) and (21) induces a spatial Hopf bifurcation to the system irrespective of the nature of the kinetics, and the kinetics parameters only determine the value of τ at the bifurcation point. In contrast to Turing instability, which is always associated with a finite number of wave vectors (as illustrated in Fig. 4 for the model described in Sec. III A), here all the modes above a threshold become unstable. Horsthemke derived a similar condition for spatial Hopf bifurcation in the case of a direction-independent persistent random-walk model but there the instability condition additionally requires the rate of activation to be greater than the death rate in the steady state which generally does not occur in most of the commonly studied reaction-diffusion models [11]. No such criterion on kinetic parameters limits the applicability of the analysis here and therefore the kind of instability we discuss now is expected to be manifested by many of the available reaction-diffusion models in wider ranges of parameter space. The kinetic parameter, however, determines (i) the critical value of the diffusive memory [by Eqs. (20) or (21)] above which instability is possible and
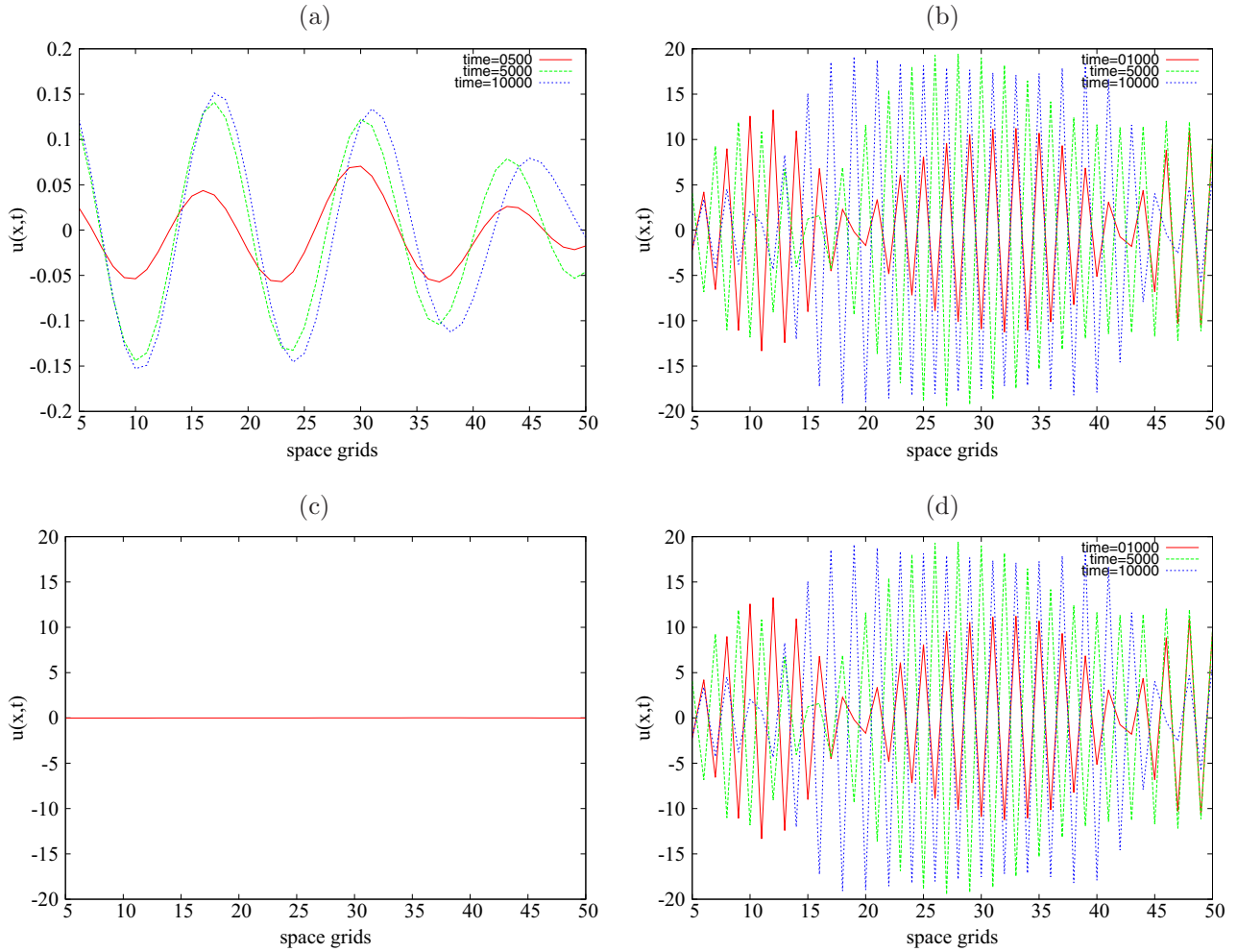
FIG. 3. Figure demonstrates the spatial distribution of the variable $u(x, t)$ simulated numerically using Eqs. (22) for the parameter space: $\alpha = 0.899$, $\beta = -0.91$, $\gamma = -0.899$, $\delta = 2.0$ and (a) $d = 1.0$, $\tau = 0.0$; (b) $d = 0.17$, $\tau = 1.0$; (c) $d = 0.516$, $\tau = 0.0$; and (d) $d = 0.516$, $\tau = 0.34$, at three arbitrarily chosen time instants. In (a) and (c) the diffusive memory is not considered. Panel (a) corresponds to a Turing region, the concentration is always nonuniform in space, and the distribution reaches stationarity in quick time, producing a stationary Turing structure. Panel (c), on the other hand, corresponds to parameter space beyond the Turing zone, and the concentration reaches uniformity throughout the space in quick time. Panels (b) and (d) are the results of simulation when diffusive memory is considered and has a value higher than the threshold inside Turing region and beyond it, respectively. Evidently diffusive memory induces a complex spatial structure which keep changing in time, never reaching stationarity. This suggests the memory induces a spatial Hopf bifurcation. Since the distribution of concentration in space keep evolving in time, we get a spatial structure that keep changing in time; a complicated spatiotemporal structure as demonstrated in Fig. 1.

(ii) the threshold wave vector [by Eq. (17)]. In the section that follows we numerically simulate two reaction-diffusion models, commonly studied in thi context of pattern formation, in the presence of diffusive memory in order to (i) verify how far the analytic predictions are met through numerical simulation and to (ii) ascertain the nature of the Hopf bifurcation, i.e., whether it is supercritical or subcritical.

III. NUMERICAL SIMULATIONS

The results of linear analysis strictly holds for the initial phases of a dynamics when the perturbation is still small. The linearization scheme fails as the perturbation grows and its predictions often go wrong in the long-time limit. So a linear stability analysis must always be accompanied by numerical investigations. For dynamical models that include memory or inertia, the numerical results are particularly important because though instances of dynamical delay inducing long-time stable spatial structures are well known, the effect of inertia on the dynamics often dies down in the long run. Further, a Hopf bifurcation could be either subcritical or supercritical, where a supercritical bifurcation is characterized by small-amplitude limit-cycle oscillation while a supercritical one may lead to a potentially dangerous large-amplitude oscillation diverging away to infinity or chaos. A straightforward prescription to ascertain whether the bifurcation is subcritical or supercritical in nature is to numerically simulate the model to check for the appearance of a small-amplitude limit cycle near the bifurcation point.

In this section we present a numerical analysis on two prototype reaction-diffusion models and compare the results both with and without diffusive memory. The model
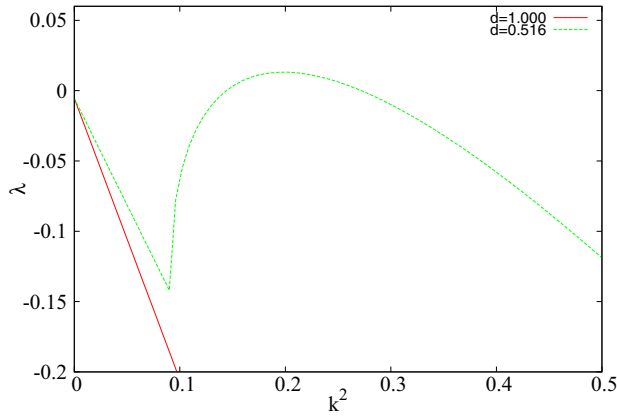
FIG. 4. Dispersion diagram for the model given by Eqs. (22) for the parameter space: $\alpha = 0.899$, $\beta = -0.91$, $\gamma = -0.899$, $\delta = 2.0$, and d as mentioned in the figure.

dynamics were simulated using XPPAUT software which employs fourth-order Ranga-Kutta to solve both the ordinary partial and the delayed partial differential equations. In every case the initial conditions are set by subjecting the dynamical variables $u(x,t)$ and $v(x,t)$ to random perturbations around the respective steady states (u_0 and v_0) (random perturbations generated by the Box-Muller algorithm).

A. Pigmentation fish model

First, we consider the generic reaction-diffusion model proposed by Bario *et al.* [26], given as

$$u_t(x,t) = \alpha u(1 - r_1 v^2) + v(1 - r_2 u) + \delta d \nabla^2 u(x, t - \tau),$$
$$v_t(x,t) = \beta v(1 + \alpha r_1 u v / \beta) + v(\gamma + r_2 v) + \delta \nabla^2 v(x,t).$$
(22)

Here α, β, γ, r_1, and r_2 are kinetic parameters; δ defines the length scale of the system; and d is the ratio of the diffusion coefficients of the two species. The reaction terms in this model are not phenomenological, but rather their choice is guided by the requirement of conservation of certain chemicals and the nonlinearity is chosen to determine specific unstable modes to dominate for the selection of a particular type of pattern under Turing conditions. Due to its generalized structure, the model has been employed to study several attributes of Turing pattern [27]. The condition $\alpha = -\gamma$ ensures the (0,0) to be the only spatially uniform steady state of the system while $\alpha + \beta < 0$; $\alpha\beta - \gamma > 0$ ensures that the homogeneous state is stable. At $d > -\frac{\alpha}{\beta}$ the state loses its stability to inhomogeneous perturbation and a Turing pattern is formed. We intend to explore the effect of the introduction of diffusive memory numerically on the spatiotemporal dynamics in both the Turing region and beyond, since condition (17) could be satisfied at above given thresholds of k for both the cases. Computations are performed on Eq. (22) by an explicit Euler method on a one-dimensional grid with 100 data points with $\Delta x = 1.0$ and time step $\Delta t = 1.0 \times 10^{-4}$ under zero flux boundary conditions using the software XPPAUT. Results of the simulation are shown in Figures 1, 2, and 3. Figures 1(a) and 1(b) give the space-time contours of the
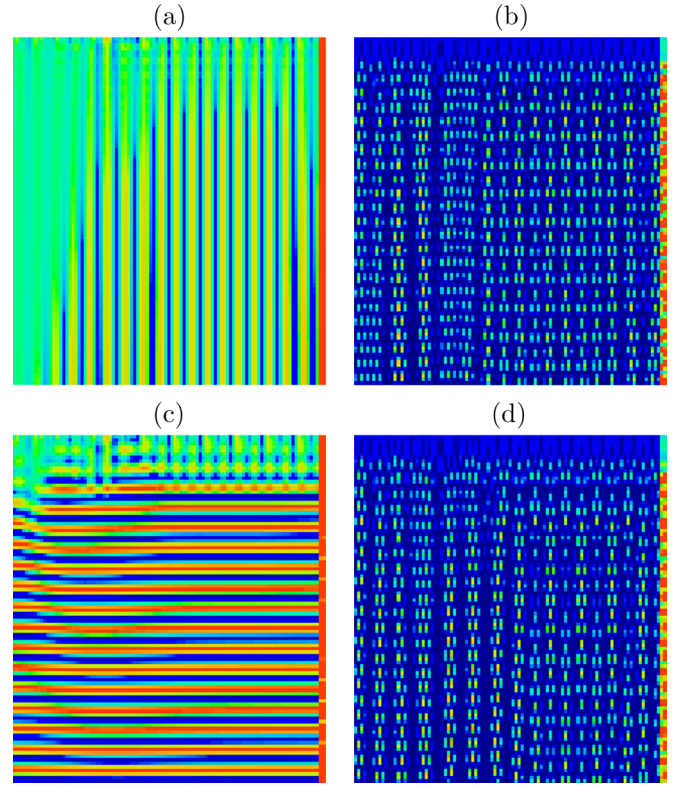

FIG. 5. Figure demonstrates the space-time contour of the the variable $u(x,t)$ simulated numerically using Eqs. (23) for the parameter space: $a = 18.0$, $b = 1.5$, $d = 1.6$, and (a) $\sigma = 8.0$, $\tau = 0.0$; (b) $\sigma = 8.0$, $\tau = 1.0$; (c) $\sigma = 4.0$, $\tau = 0.0$; (d) $\sigma = 4.0$, $\tau = 1.0$. Panels (a) and (c) give the concentration distribution when the diffusive memory is not considered. Panel (a) corresponds to a Turing region, and time is plotted along the y axis so the perpendicular stripes represent a stationary Turing structure. Panel (c) corresponds to a Hopf region, and the horizontal stripes represent homogeneous oscillations. Panels (b) and (d) are the results of simulation when diffusive memory is considered and has a value higher than the threshold in the Turing and Hopf regions, respectively. In both the cases the inclusion of diffusive memory induces a spatiotemporal structure, suggesting simultaneous occurrence of spatial inhomogeneity and temporal nonstationarity. The nature of the temporal and spatial structure would be separately demonstrated in Figs. 6 and 7, respectively.

concentration variable $u(x,t)$ according to Eq. (22) in a parameter zone beyond the Turing bifurcation in the absence and in the presence of diffusive memory, respectively. Figures 1(c) and 1(d) depict the same for a parameter region within the Turing space. Spatiotemporal instability arises from spatially homogeneous and inhomogeneous states respectively in the two cases above a threshold value of the diffusive memory. The values of τ required to switch on the spatiotemporal instability in the two cases are different (as argued in Sec. II): 0.32 and 0.17 for the unstable (Turing) and stable regions, respectively. For easy understanding of the nature of bifurcation, I plot $u(x,t)$ against time and space, respectively, in Figs. 2 and 3. Figures 2(a) and 2(b) correspond to the temporal evolution in the Turing region of the parameter space, without and with delay while Figs. 2(c) and 2(d) show the same beyond it. The
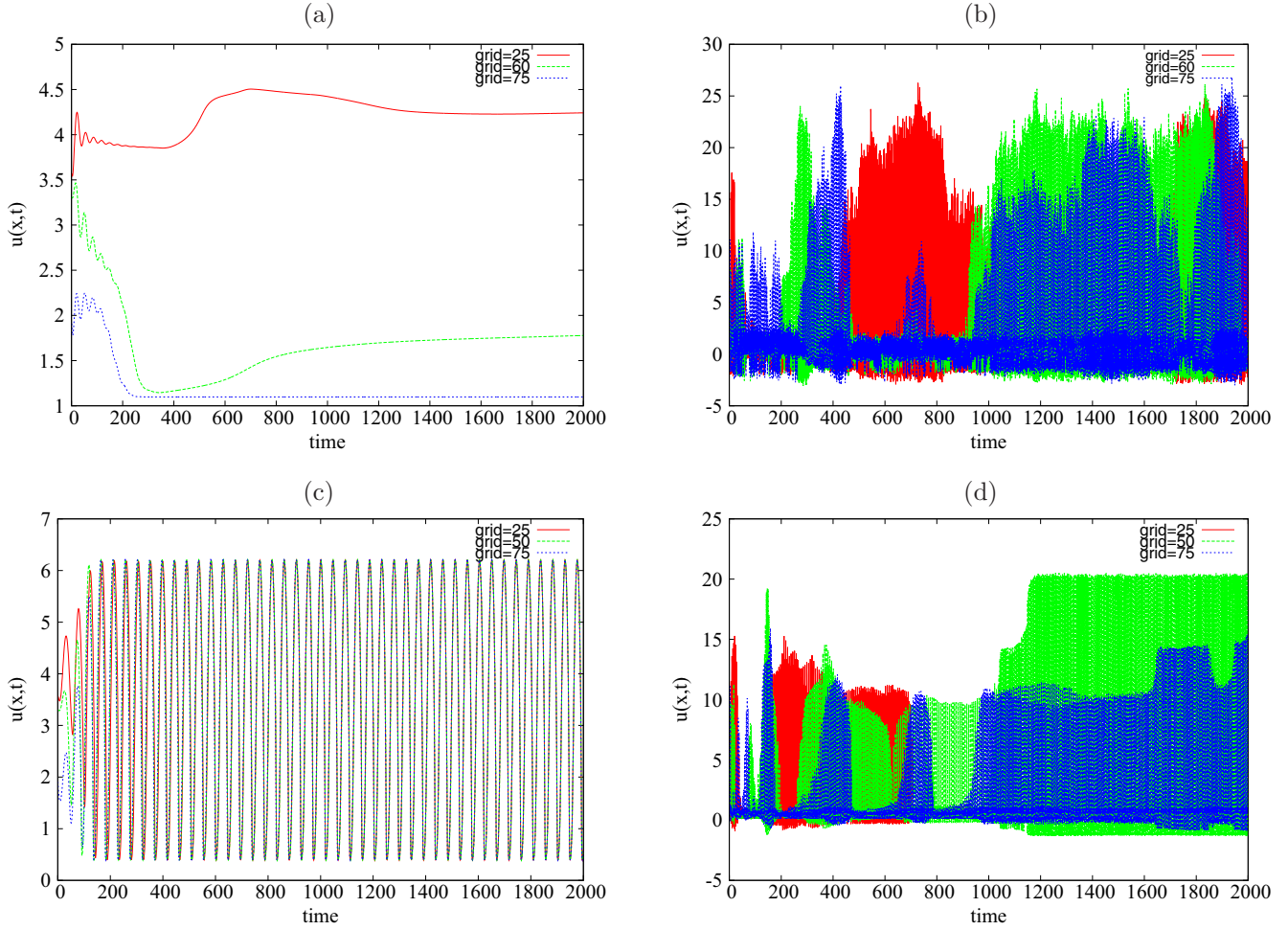
FIG. 6. Figure demonstrates the temporal evolution of the variable $u(x, t)$ simulated numerically using Eqs. (23) for the parameter space: $a = 18.0, b = 1.5, d = 1.6$, and (a) $\sigma = 8.0, \tau = 0.0$; (b) $\sigma = 8.0, \tau = 1.0$; (c) $\sigma = 4.0, \tau = 0.0$; and (d) $\sigma = 4.0, \tau = 1.0$, at three arbitrarily chosen grid points. Panels (a) and (c) give the concentration distribution when the diffusive memory is not considered. Panel (a) corresponds to a Turing region, and the concentration at the three points reaches stationarity but each at a different value, as required for a stationary Turing structure. Panel (c), on the other hand, corresponds to a Hopf region, characterized by homogeneous oscillation in the concentration variables. Panels (b) and (d) are the results of simulation when diffusive memory is present and has a value higher than the threshold in the Turing and Hopf regions, respectively. Evidently diffusive memory generates a complex temporal oscillation in the concentration variables which is also inhomogeneous in space. This suggests the diffusive memory induces a supercritical Hopf bifurcation. As the amplitudes of oscillation is not uniform in space, we obtain a spatial structure that keep changing in time; a complicated spatiotemporal structure as demonstrated in Fig. 5.

temporal oscillation observed in Figs. 2(b) and 2(d) indicates a Hopf bifurcation. Similarly, Figs. 3(a) and 3(b) correspond to the spatial variation of $u(x, t)$ in the Turing region, without and with memory; while Figs. 3(c) and 3(d) show the same beyond it. Evidently delay induces a spatial structure in both cases. Notably, the irregular nature of the spatial structure in presence of memory reflects the presence of a large number of unstable modes [by condition (17) all modes above a threshold k are unstable in the presence of delay]. This is in sharp contrast to the regular Turing structures indicative of a finite number of unstable modes (a typical dispersive behavior is demonstrated in the Fig. 4). Thus the inclusion of a diffusive memory in the dynamics is capable of inducing a spatial Hopf bifurcation to a model which otherwise never shows any kind of temporal instability. Further, a spatial inhomogeneity is generated here in spite of the ratio of the diffusion coefficients being unity (a condition necessary for spatial structures to be

formed according to Turing's theory). Earlier studies on the model did show generation of spatial patterns under such a condition but only in the presence of external fields [27].

B. CIMA model

Now I consider the case of the well-known chlorite-iodide-malonic acid model. The model is given in terms of two concentration variables and can be described by the following pair of partial differential equations:

$$u_t(x, t) = a - u - \frac{4uv}{1 + u^2} + \nabla^2 u(x, t - \tau)$$

$$v_t(x, t) = \sigma \left[b \left(u - \frac{4uv}{1 + u^2} \right) + d \nabla^2 v(x, t) \right], \quad (23)$$

where $u(x, t)$ and $v(x, t)$ represent the dimensionless concentrations of the species chlorite and iodide. By changing
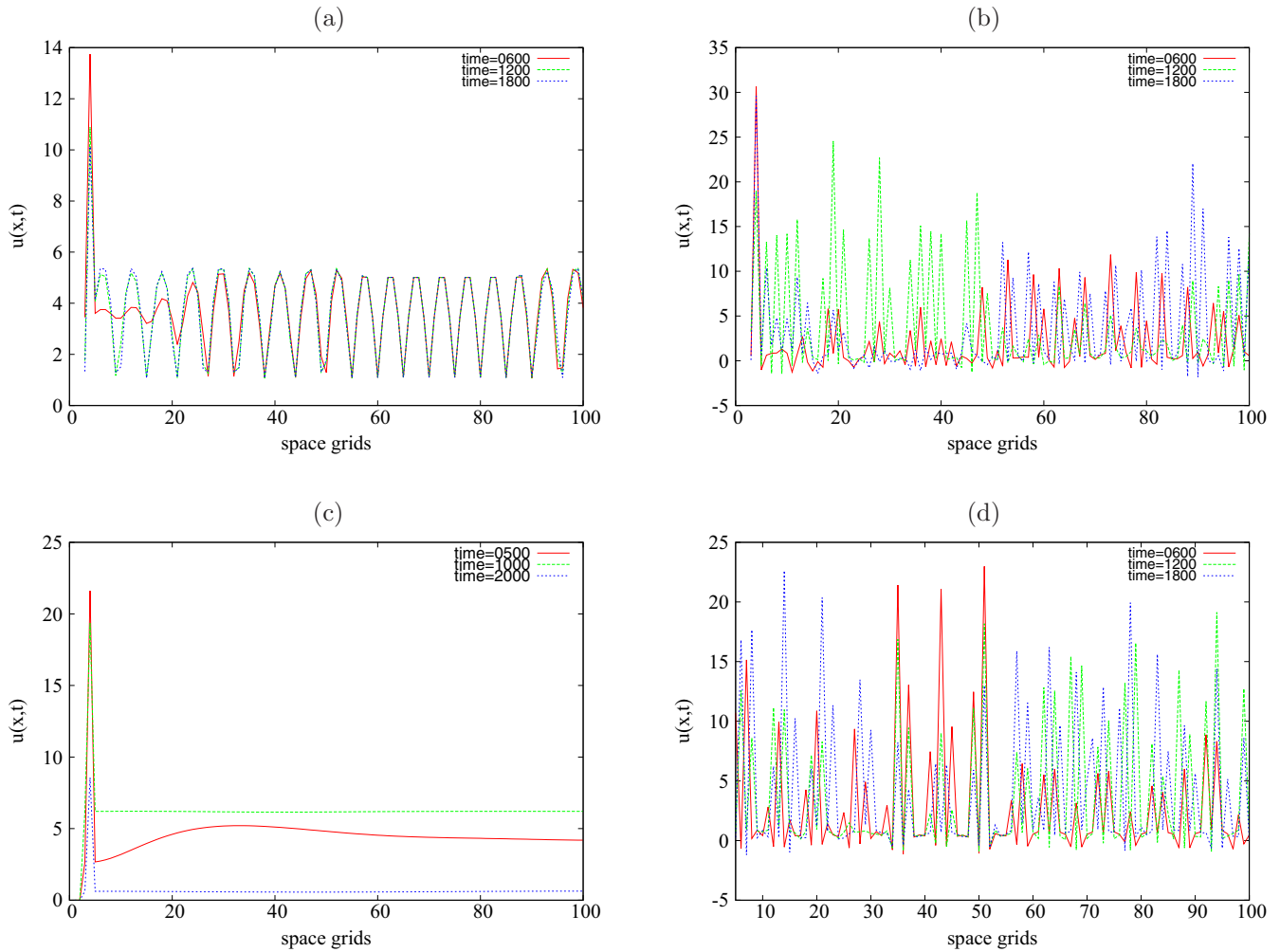
FIG. 7. Figure demonstrates the spatial distribution of the variable $u(x, t)$ simulated numerically using Eqs. (23) for the parameter space: $a = 18.0$, $b = 1.5$, $d = 1.6$, and (a) $\sigma = 8.0$, $\tau = 0.0$; (b) $\sigma = 8.0$, $\tau = 1.0$; (c) $\sigma = 4.0$, $\tau = 0.0$; (d) $\sigma = 4.0$, $\tau = 1.0$, at three arbitrarily chosen time instants. In (a) and (c) the diffusive memory is not considered. Panel (a) corresponds to a Turing region, the distribution is always inhomogeneous in space, and initially nonstationary but eventually evolves to an equilibrium distribution producing a stationary Turing structure. Panel (c) corresponds to the Hopf region of parameter space, and the concentration reaches a uniform value throughout the space and this value periodically changes in time. Panels (b) and (d) are the results of simulation when diffusive memory is present and has a value higher than the threshold in the Turing and Hopf regions, respectively. Evidently diffusive memory in each of the cases generates a complex spatial structure that keeps changing in time, never reaching stationarity. This suggests the memory induces a spatial Hopf bifurcation. Since the spatial distribution of concentration continually evolve in time, we get the complicated spatiotemporal structure demonstrated in Fig. 5.

the value of the parameter σ which denotes the concentration of starch present in the reaction medium, one can switch between pure Hopf and pure Turing modes. Historically, a Turing pattern was first experimentally demonstrated in this chlorite-iodide-malonic acid model [28–30] thanks to the model fulfilling the instability criteria of inhibitor diffusing faster than the activator due to the formation of a starch-iodide complex which renders the iodide slow-moving compared to chlorite [31]. Since then, this model has been extensively applied both for theoretical and experimental studies, like in the investigation of Turing patterns under external influence [32–35], the appearance of spirals [36], generation of spatial periodicity [21] or the existence of Hopf-Turing mixed modes [37]. Here we consider the effect of diffusive memory on the dynamics at two different parameter regions, corresponding to a pure Hopf and pure Turing, respectively. In both the cases

it is always possible to satisfy the condition (17) above a threshold value of k. [It is worthwhile to mention here that the direction-independent reaction-walk model precludes the spatial Hopf instability in this model since here the required condition $A_{11} - d(u_0, v_0)$ can never be satisfied.] Numerically, we solve Eqs. (23) using XPPAUT in a one-dimensional grid of 100 data points with $\Delta x = 1.0$ space points and time steps $\Delta t = 0.05$ under zero flux boundary condition. The results of the simulation are presented in Figs. 5, 6, and 7. Figures 5(a) and 5(b) give the the space-time contours of the concentration variable $u(x, t)$ according to Eq. (23) in the pure Hopf region of parameter space, in the absence and in the presence of memory, respectively. Evidently homogeneous oscillation gives way to complex spatiotemporal structures in the presence of memory indicating the occurrence of spatial Hopf bifurcation. The values of τ required to switch on the
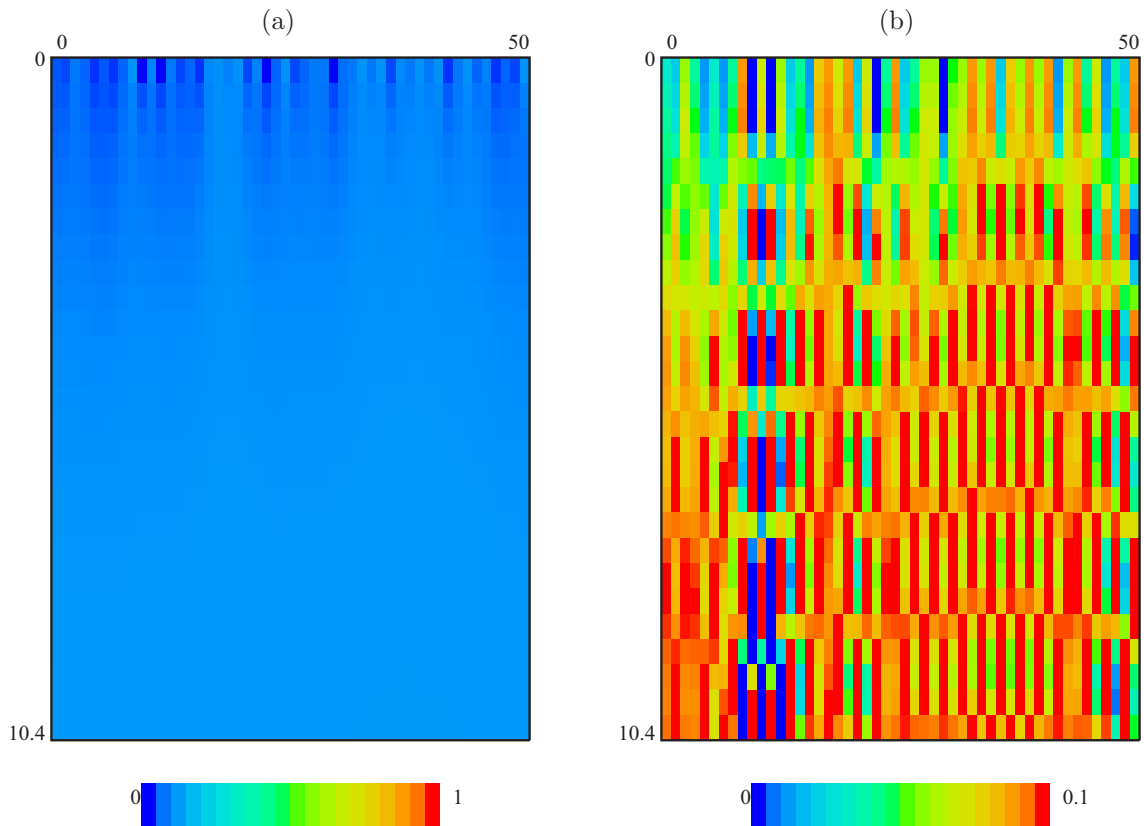
FIG. 8. Figure demonstrates the space-time contour of the the variable $u(x, t)$ simulated numerically using Eqs. (25) for the parameter space: $r = 0.5$, ak $= 0.1$, $d = 0.5$ along with (a) $\tau = 0$, (b) $\tau = 1.0$. Panel (a) corresponds to a parameter space beyond the Turing zone, marked by a uniform distribution of species in space and time. Panel (b) gives the concentration distribution in the same parameter region with the delay switched on. Thus the inclusion of diffusive memory induces a spatiotemporal structure on an otherwise homogeneous distribution, this suggests the simultaneous occurrence of spatial inhomogeneity and temporal nonstationarity induced by the memory. The nature of the temporal and spatial structure are separately demonstrated in Figs. 9 and 10, respectively.
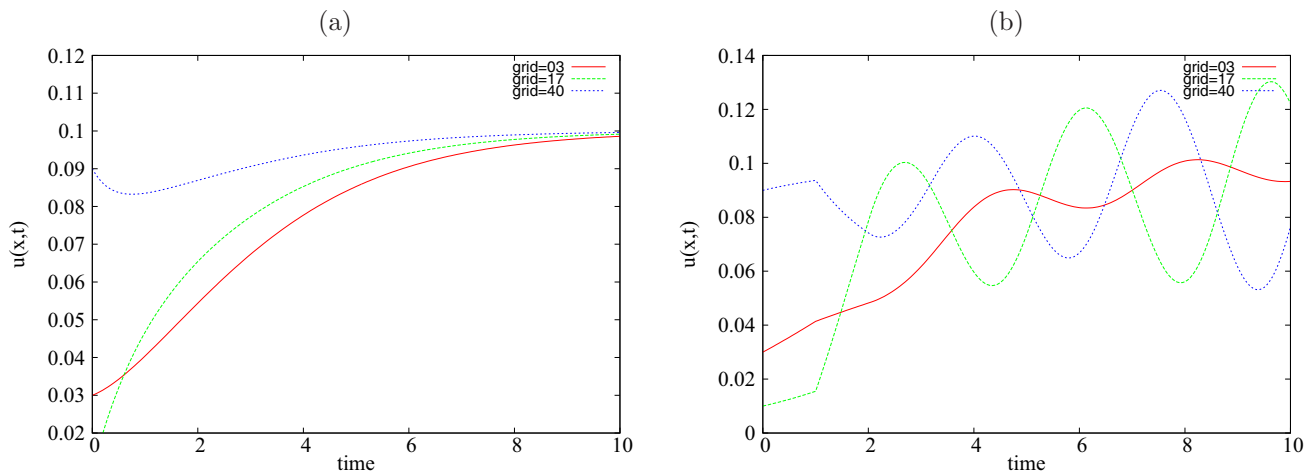

FIG. 9. The time evolution of the the variable $u(x, t)$ simulated numerically using Eqs. (25) for the parameter space: $r = 0.5$, ak $= 0.1$, $d = 0.5$ along with (a) $\tau = 0$ (b) $\tau = 1.0$. Panel (a) corresponds to a stable zone of the parameter space, marked by the species reaching stationarity at same value in all the three arbitrarily chosen space points. Panel (b) gives the time evolution of $u(x, t)$ in the same parameter region with the delay switched on. Evidently diffusive memory induces a complex temporal oscillation in the concentration variables in all the three cases. This suggests the diffusive memory induces a Hopf bifurcation. The phase or the amplitudes of oscillation are not synchronized for the three space points, therefore we get a spatial structure that keeps changing in time, a complicated spatiotemporal structure as demonstrated in Fig. 8.
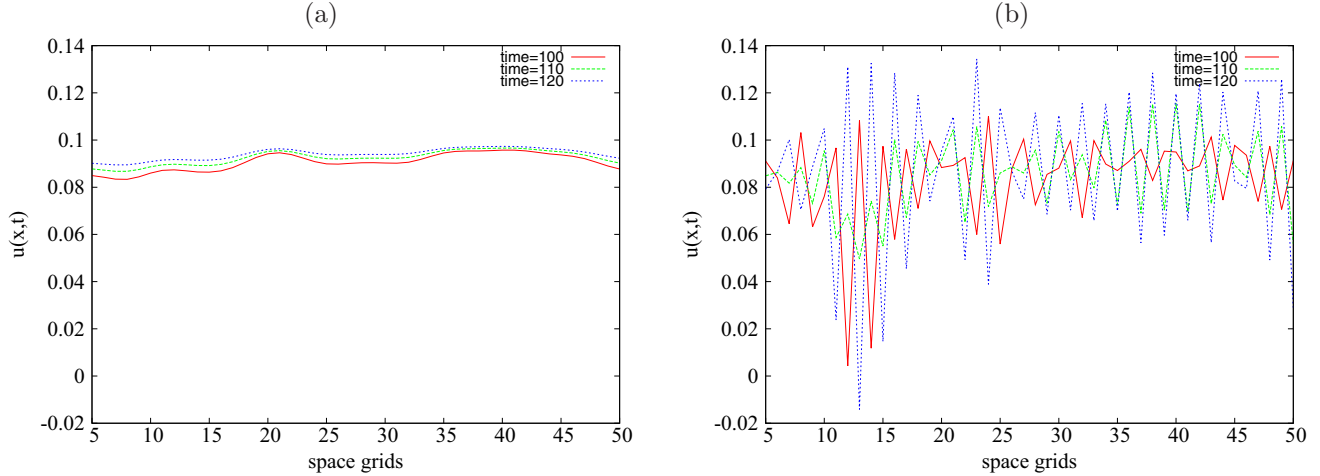
FIG. 10. Figure demonstrates the spatial distribution of the the variable $u(x, t)$ simulated numerically using Eqs. (25) for the parameter space: $r = 0.5$, ak=0.1, $d = 0.5$ along with (a) $\tau = 0$ (b) $\tau = 1.0$ at three arbitrarily chosen time instants. Panel (a) corresponds to a stable zone of the parameter space, marked by the species reaching uniform value throughout the space. Panel (b) gives the spatial distribution of $u(x, t)$ in the same parameter region with the delay switched on. Evidently diffusive memory generates a complex spatial structure that keeps changing in time, never reaching stationarity. This suggests that the memory induces a spatial Hopf bifurcation. Since the spatial distribution of concentration continually evolves in time, we get the complicated spatiotemporal structure demonstrated in Fig. 5.

spatiotemporal instability in the two cases are different [due to the dependence of threshold τ on the kinetic parameters by Eqs. (20) and (21)]; 0.8 and 0.3 for the unstable (Hopf) and unstable (Turing) region, respectively. Figures 5(c) and 5(d) depict the spatiotemporal distribution of concentration for a parameter region within the Turing space. Here a spatiotemporal structure is produced induced by the diffusive memory at the cost of the stationary spatial pattern. For easy understanding of the nature of the nature of bifurcation, I have plotted the value of $u(x, t)$ against time and space, respectively, in Figs. 6 and 7. Figures 6(a) and 6(b) corresponds to the temporal evolution in the Hopf region of the parameter space, without and with delay, while Figs. 6(c) and 6(d) show the same in a Turing space. The temporal oscillation observed in Figs. 6(b) and 6(d) is a clear indicator of a Hopf bifurcation. Similarly, Figs. 7(a) and 7(b) correspond to the spatial variation of $u(x, t)$ in the Turing region, without and with delay, while Figs. 7(c) and 7(d) show the same beyond it. Evidently delay induces a spatial structure in both cases.

C. Fisher model

Before we conclude this section, here I briefly mention the results of numerical analysis with the well-known Fisher model. Originally proposed for propagation of an advantageous allele in the distribution of genes, the Fisher model and its many variants have found wide applicability in fields ranging from ecology, physiology, combustion, crystallization, plasma physics, and in general phase transition problems. The one-variable Fisher model consists of a birth-death process with logistic population growth term for the species along with the diffusion

$$u_t(x, t) = ru(1 - u/k) + d\nabla^2 u(x, t). \qquad (24)$$

Here r denotes the linear growth rate and k the carrying capacity of the species. Considering memory in the diffusion

(which implies these species require a finite time to respond to a gradient of population density) we write

$$u_t(x, t) = ru(1 - u/k) + d\nabla^2 u(x, t - \tau). \qquad (25)$$

Equation (25) is now solved by an explicit Euler method on a one-dimensional grid with 50 space points with $\Delta x = 1.0$ and time step $\Delta t = 1.0 \times 10^{-4}$ under zero flux boundary condition using the software XPPAUT. Results of the simulation are shown in the Fig. 8. Figures 8(a) and 8(b) give the space-time contours of the concentration variable $u(x, t)$ according to Eq. (25) in a parameter zone that corresponds to a stable state in the absence of memory. Figures 9 and 10 describe the temporal and spatial variation of the concentration variable respectively. Spatiotemporal instability arises out of spatially homogeneous state above a threshold value of the diffusive memory. (I did not produce any more detailed results of the model in other parameter regions for fear of repetition).

IV. CONCLUSION

Cattaneo's modification of Fick's law of diffusion is in general based on linearization of the delayed flux around the current time and therefore not always applicable when the inertia is large. Instead, here we start with the form of reaction-diffusion model, which includes a memory in the diffusion part, to arrive at a condition for spatial Hopf bifurcation, induced by the diffusive memory. Analysis suggests the system loses stability due to all the wave vectors above a minimum crossing the instability threshold, when the diffusive memory (that is the inertia) is sufficiently large. The stability criteria does not impose any restriction on the kinetic parameters (which only determines the critical value of the diffusive memory and also the minimum wave vector) and therefore can easily be realized in common reaction-diffusion systems. This is in contrast to an earlier work by Horsthemke [11] which employs a microscopic approach to demonstrate

that such a spatial Hopf instability would be suppressed by the kinetics in most of the commonly studied reaction-diffusion models. The results of the analysis in our case is vindicated by numerical investigation with three prototype reaction-diffusion models which includes a real chemical, a generalized pattern forming, and one ecological model. In all the cases inclusion of diffusive memory leads to spatiotemporal oscillations; in the first two models the oscillations at each space point stabilize to finite small amplitude limit cycles suggesting the Hopf bifurcation involved to be supercritical in nature. In the other model the oscillations keep growing and eventually the dynamics diverge in the long run, which indicates that the instability is subcritical Hopf. The oscillations in different space points are not synchronized to each other and the simultaneous occurrence of temporal oscillation and spatial inhomogeneity produce a spatial structure which keeps changing in time. The irregular structure of the spatiotemporal distribution at any time instant here reflects the presence of a large number of unstable modes, in contrast to regular Turing patterns which are characterized by only a few unstable wave vectors. Spatiotemporal structures are a common occurrence in a wide range of chemical, physical, and biological models. While a number of mechanisms have been put forward to account for the generation of these patterns, in many cases stringent instability criteria on the kinetic parameters limits their applicability. The significantly lenient stability criteria for the mechanism proposed here therefore could bring a wider range of pattern-forming phenomena to mathematical modeling.

ACKNOWLEDGMENTS

[1] C. Cattaneo, C. R. Acad. Sci. Paris **247**, 431 (1958).

[2] T. Ruggeri, A. Muracchini, and L. Seccia, Phys. Rev. Lett. **64**, 2640 (1990).

[3] J. J. Bissell, Proc. R. Soc. London, Ser. A **471**, 20140845 (2015).

[4] M. Zakari and D. Jou, Phys. Rev. D **48**, 1597 (1993).

[5] J. B. D. Pavon and D. Jou, Class. Quantum Grav. **8**, 347 (1991).

[6] H. P. D. Oliveira and J. M. Salim, Acta Phys. Pol. B **19**, 649 (1988).

[7] V. Mendez, S. Fedotov, and W. Horsthemke, *Reaction-Transport Systems Mesoscopic Foundations, Fronts, and Spatial Instabilities* (Springer, Berlin, 2010), pp. 33–53.

[8] R. Furth, Z. Phys. **2**, 244 (1920).

[9] W. Kaminski, J. Heat Transfer **112**, 555 (1990).

[10] D. Campos and V. Méndez, J. Phys. A: Math. Theor. **42**, 075003 (2009).

[11] W. Horsthemke, Phys. Rev. E **60**, 2651 (1999).

[12] W. Alharbi and S. Petrovskii, Mathematics **6**, 59 (2018).

[13] J. Rodríguez-González, M. Santillan, A. Fowler, and M. C. Mackey, J. Theor. Biol. **248**, 37 (2007).

[14] C. Foley and M. C. Mackey, J. Math. Biol. **58**, 285 (2009).

[15] Z. Wang and T. Chu, Chaos, Solitons Fractals **28**, 161 (2006).

[16] X. Han, F. Xia, P. Ji, Q. Bi, and J. Kurths, Commun.. Nonlin. Sci. Numer. Simul. **36**, 517 (2016).

[17] D. Ding, J. Zhu, X. Luo, and Y. Liu, Nonlinear Anal.: Real World Appl. **10**, 2873 (2009).

[18] S. Sen, P. Ghosh, S. S. Riaz, and D. S. Ray, Phys. Rev. E **80**, 046212 (2009).

[19] H. Viktor, G. P. Luigi, V. V. K., and E. I. R., Angew. Chem., Int. Ed. **51**, 6878 (2012).

[20] A. Arneodo and J. Elezgaray, Phys. Lett. A **143**, 25 (1990).

[21] S. Sen, P. Ghosh, S. S. Riaz, and D. S. Ray, Phys. Rev. E **81**, 017101 (2010).

[22] A. De Wit, *Spatial Patterns and Spatiotemporal Dynamics in Chemical Systems* (John Wiley & Sons, Inc., New Jersey, 2007), pp. 435–513.

[23] E. V. H. Malchow and S. V. Petrovskii, *Spatiotemporal Patterns in Ecology and Epidemiology: Theory, Models, and Simulation* (Chapman & Hall/CRC, London, 2007).

[24] V. K. Jirsa and J. A. S. Kelso, Phys. Rev. E **62**, 8462 (2000).

[25] M. Adimy, F. Crauste, and S. Ruan, J. Theor. Biol. **242**, 288 (2006).

[26] R. Barrio, C. Varea, J. Aragón, and P. Maini, Bull. Math. Biol. **61**, 483 (1999).

[27] S. S. Riaz, S. Kar, and D. S. Ray, J. Chem. Phys. **121**, 5395 (2004).

[28] P. D. Kepper, V. Castets, E. Dulos, and J. Boissonade, Physica D **49**, 161 (1991).

[29] Q. Ouyang and H. L. Swinney, Nature **352**, 610 (1991).

[30] V. Castets, E. Dulos, J. Boissonade, and P. De Kepper, Phys. Rev. Lett. **64**, 2953 (1990).

[31] I. Lengyel and I. R. Epstein, Science **251**, 650 (1991), .

[32] M. Dolnik, A. M. Zhabotinsky, and I. R. Epstein, Phys. Rev. E **63**, 026101 (2001).

[33] P. Ghosh, S. Sen, S. S. Riaz, and D. S. Ray, Phys. Rev. E **79**, 056216 (2009).

[34] S. S. Riaz, S. Dutta, S. Kar, and D. S. Ray, Eur. Phys. J. B **47**, 255 (2005).

[35] S. S. Riaz, S. Kar, and D. S. Ray, Physica D **203**, 224 (2005).

[36] S. S. Riaz and D. S. Ray, J. Chem. Phys. **123**, 174506 (2005).

[37] C. M. Topaz and A. J. Catllá, Phys. Rev. E **81**, 026213 (2010).